

First principles investigation of exchange interactions in quasi-one-dimensional antiferromagnet CaV_2O_4

Z.V. Pchelkina^{1,2,*} and I. V. Solovye^{2,3,†}

¹*Institute of Metal Physics, S.Kovalevskoy St. 18, 620990 Ekaterinburg, Russia*

²*Ural Federal University, Mira St. 19, 620002 Ekaterinburg, Russia*

³*Computational Materials Science Unit,*

National Institute for Materials Science,

1-1 Namiki, Tsukuba, Ibaraki 305-0044, Japan

(Dated: October 26, 2018)

Abstract

The effect of orbital degrees of freedom on the exchange interactions in the spin-1 quasi-one-dimensional antiferromagnet CaV_2O_4 is systematically studied. For this purpose a realistic low-energy model with the parameters derived from the first-principles calculations is constructed. The exchange interactions are calculated using both the theory of infinitesimal spin rotations near the mean-field ground state and the superexchange model, which provide a consistent description. The obtained behavior of exchange interactions substantially differs from the previously proposed phenomenological picture based on the magnetic measurements and structural considerations, namely: (i) Despite quasi-one-dimensional character of the crystal structure, consisting of the zigzag chains of edge-sharing VO_6 octahedra, the electronic structure is essentially three-dimensional, that leads to finite interactions between the chains; (ii) The exchange interactions along the legs of the chains appear to dominate; and (iii) There is a substantial difference of exchange interactions in two crystallographically inequivalent chains. The combination of these three factors successfully reproduces the behavior of experimental magnetic susceptibility.

PACS numbers: 71.20.-b, 71.70.Gm, 75.30.Et

I. INTRODUCTION

The CaV_2O_4 compound was studied both theoretically and experimentally owing to its low-dimensional magnetism and frustrated structure¹⁻³. The high temperature orthorhombic phase (the space group $Pnam$) undergoes the phase transition into low temperature monoclinic phase (the space group $P2_1/n11$) at $T_s \approx 141$ K. The main motif of both structures is zigzag double chains of edge-sharing VO_6 octahedra (see figure 1). The distances between nearest and next-nearest V neighbors are nearly equal, which together with the antiferromagnetic (AFM) type of interactions gives rise to the geometrical frustration. The electronic configuration of V^{3+} is $3d^2$, making CaV_2O_4 the appropriate compound for investigation of $S=1$ quasi-one-dimensional magnetism.

CaV_2O_4 has two crystallographically inequivalent types of vanadium atoms, V1 and V2, forming the zigzag chains. The vanadium atoms are displaced out of the center of octahedra (figure 1 of supplementary material available at⁴), yielding the existence of finite electric dipoles. However, both structures possess the inversion symmetry, meaning that the dipoles are ordered antiferroelectrically. Each zigzag chain propagates along the a axis and has two neighboring chains of other type, which are stacked along c and b axes (see figures 1(b) and 1(c), respectively). Each vanadium atom has six nearest vanadium neighbors forming six main exchange paths (the notations of corresponding interatomic distances are given in the brackets): J_1^l and J_2^l (d_1^l and d_2^l) - along the “leg” of the chain formed by V1 and V2, respectively; J_1^+ , J_1^- and J_2^+ , J_2^- (d_1^+ , d_1^- and d_2^+ , d_2^-) - along the zigzag in the positive and negative direction of a (denoted by “+” and “-”, respectively); and two groups of interchain interactions along c and b : (J_c^+ , J_c^-) and (J_b^+ , J_b^-), respectively (see figure 1).

The magnetic structure of CaV_2O_4 have been studied already in 70’s^{5,6} but it was impossible in that time to resolve the low temperature monoclinic crystal structure and analyze correctly experimental data. It is well known that below $T_N \approx 51-78$ K the long range antiferromagnetic order with a propagation vector $\mathbf{k} = (0, \frac{1}{2}, \frac{1}{2})$ sets in^{2,5-8}. The reduction of magnetic moment $1.0\mu_B \leq m \leq 1.59\mu_B$ was detected in ^{51}V nuclear magnetic resonance (NMR) measurements, muon-spin spectroscopy investigations and powder diffraction^{2,5-8}. The collinear spin orientation was found in the first neutron powder diffraction experiments at low temperatures^{5,6}. However, it was questioned in more recent NMR measurements⁸ and neutron diffraction experiments on high quality single crystals³, which suggest some

noncollinear spin arrangement.

Since the distances in the leg $d_{1,2}^l$ are nearly the same as in the zigzag $d_{1,2}^\pm$ (see figure 1) one could naively expect nearly equal exchange interactions $J_{1,2}^l \approx J_{1,2}^\pm$. However, the high-temperature dc susceptibility measurements of CaV_2O_4 single crystals reveal that above T_s the system behaves like a $S=1$ Heisenberg chain³. In order to explain this fact, it was typically assumed that (i) The zigzag chains, formed by V1 and V2, are nearly equivalent; and (ii) Three t_{2g} orbitals of vanadium sites are oriented in such a way that their lobes are parallel to d^l , d^+ , and d^- , giving rise to the exchange paths J^l , J^+ , and J^- , respectively (J_{leg} , J'_{zz} and J''_{zz} in the notations of³).

In the orthorhombic phase, the lowest t_{2g} orbital was supposed to be occupied by one electron, while the second electron resides on a double degenerate level³. The direct overlap of the first orbitals leads to the strong AFM interaction along the leg (J^l), while the interactions in the zigzag are identical ($J^+ = J^-$) and should be considerably weaker than J^l . Hence, the system in the orthorhombic phase could be considered as a $S=1$ Haldane chain. This scenario was supported by results of exact diagonalization calculations, supplemented with the fitting of the experimental high-temperature susceptibility data, which yield $J^l = -18.60$ meV and $J^+ = J^- = -3.02$ meV³. Nevertheless, in the same work³, yet another scenario was proposed with $J^+ = J^- = -19.85$ meV and $J^l = -0.75$ meV, which equally well fits the experimental data. In both cases, the fitting yields the Curie temperature $\Theta = -418$ K and the effective magnetic moment $\mu_{exp} = 2.77\mu_B$ ³.

Under the transition to the monoclinic phase, the additional distortions of the VO_6 octahedra completely lifts the degeneracy of t_{2g} orbitals and make all the exchange paths inequivalent. Moreover, two t_{2g} orbitals are supposed to be occupied and one orbital is empty, that should lead to the inequality $(J^l, J^+) \gg J^-$. Such magnetic structure with the strong exchange couplings along the leg and every second interaction along the zigzag corresponds to the spin-1 ladder.

The above scenario was based solely on the qualitative structural consideration without taking into account the existence of two nonequivalent types of vanadium atoms. Moreover, the assumed type of the orbital ordering was purely empirical and had no proper link to details of the crystal structure. In the present work we report theoretical investigation of electronic structure, orbital ordering and exchange interactions in CaV_2O_4 . For this purpose we construct the realistic low-energy model and derive parameters of this model

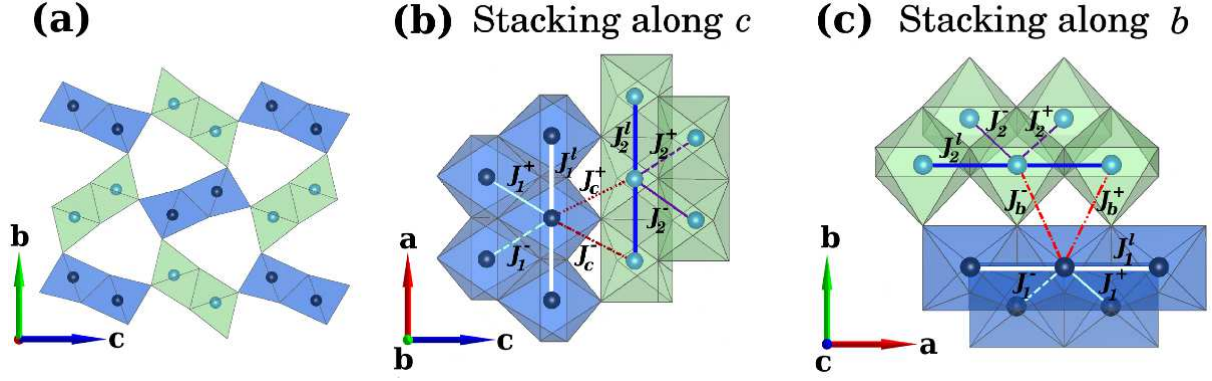


FIG. 1: (Color online) The crystal structure of monoclinic phase of CaV_2O_4 in bc , ac and ba projections. The two nonequivalent V atoms are shown as black (V1) and cyan (V2) spheres. The oxygen atoms in the corners of octahedra and the Ca atoms are not shown for simplicity. The oxygen octahedra around V1 are colored in blue, while octahedra around V2 are colored in light green. Each zigzag chain of vanadium atoms has two neighboring chains of other type, stacking along monoclinic directions c and b , as explained in panels (b) and (c), respectively. The definition of main exchange interactions for each stacking is shown. For the visualization, the VESTA software⁹ was used.

from the first-principles electronic structure calculations. Then we solve the model and obtain parameters of interatomic exchange interactions. The calculated values of exchange integrals are analyzed within superexchange theory. The spin model with the calculated exchange parameters was solved by quantum Monte-Carlo method in order to compare theoretical results with the experimental magnetic susceptibility.

II. METHOD

In order to analyze the electronic and magnetic properties of CaV_2O_4 we employ the previously developed method of “realistic modeling” (see¹⁰ for a review). The same approach has been performed for the theoretical investigation of related quasi-one-dimensional compound NaV_2O_4 ¹¹. First, the band structure of CaV_2O_4 was calculated in the local density approximation (LDA). The total and partial densities of states (DOS) for the monoclinic phase are shown in figure 2. The bands located near the Fermi level have V- t_{2g} character. Therefore, we consider the behavior of only these low-energy bands and construct for them

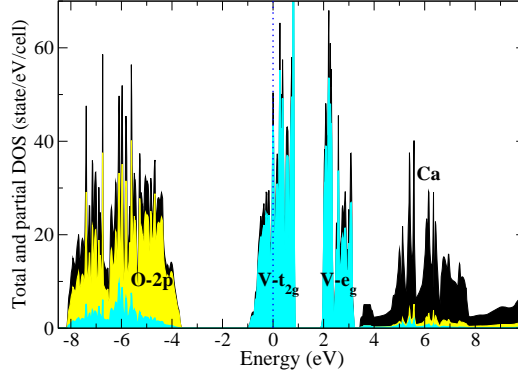


FIG. 2: (Color online) LDA total and partial densities of states for the monoclinic phase of CaV_2O_4 . The black area stands for the total DOS, yellow - for O-2p and cyan - for V-3d partial DOS. The Fermi level (dotted line) corresponds to zero.

Hubbard-type model. All parameters of this model can be derived from the first-principles electronic structure calculations in the Wannier basis. All computational details can be found in¹⁰.

Most of calculations reported in this work are performed for the experimental monoclinic $P2_1/n11$ structure (unless it is specified otherwise). We use the data from¹², but transform them to the conventional setting with the unique axis a and monoclinic angle β . The corresponding lattice parameters are $a = 2.99780 \text{ \AA}$, $b = 9.19524 \text{ \AA}$, $c = 10.68025 \text{ \AA}$ and $\beta = 90.767^\circ$, and all atomic coordinates are summarized in supplementary material available at⁴.

To construct the model one needs to specify the three sets of parameters, namely, the crystal field (CF), transfer integrals, and screened Coulomb interactions. The CF splitting of the three t_{2g} levels for the orthorhombic and monoclinic structures is shown in figure 3. The relative position of atomic t_{2g} levels in the orthorhombic phase is (0, 67, 189) meV and (0, 143, 144) meV, while in the monoclinic phase it is (0, 75, 181) meV for V1 and (0, 103, 175) meV for V1 and V2, respectively. Thus, in the orthorhombic case two of the three levels of the V2 ion are almost degenerate while in the monoclinic phase this degeneracy is lifted by the additional distortion.

The arrangement of these three t_{2g} orbitals in monoclinic phase of CaV_2O_4 corresponding to the aforementioned crystal field levels is illustrated in figure 4 in global coordinate frame.

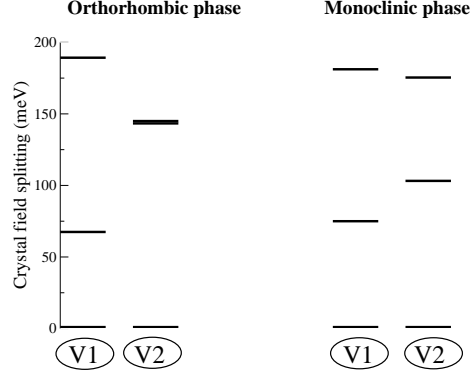


FIG. 3: The crystal field splitting of three t_{2g} states (in meV) for two types of V atoms in orthorhombic (left) and monoclinic (right) structures of CaV_2O_4 .

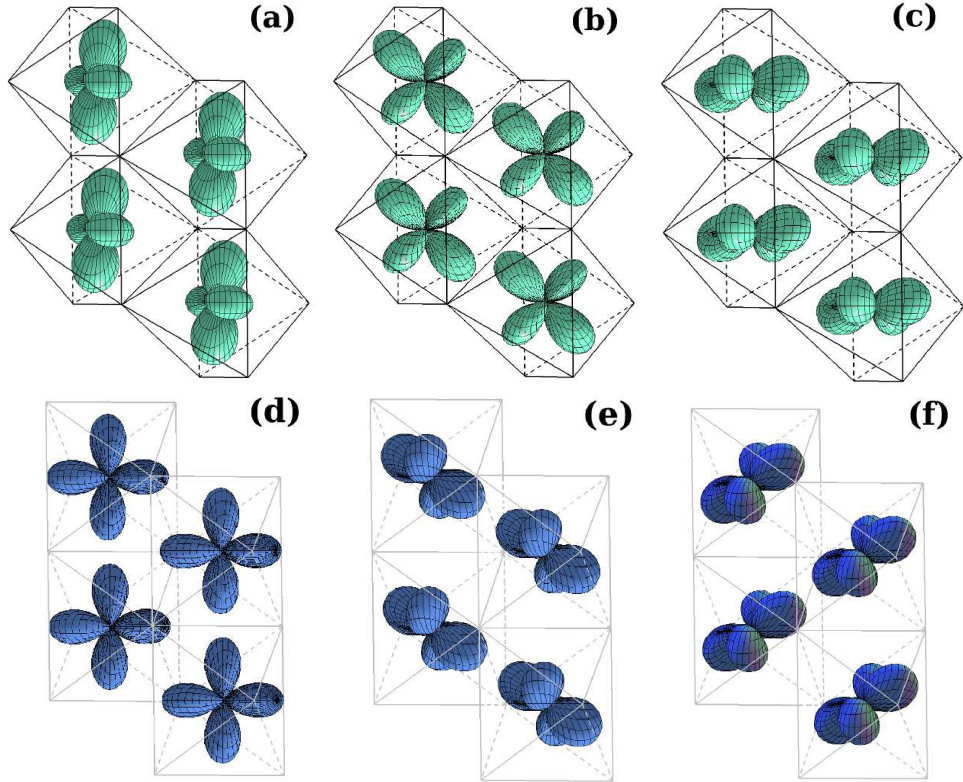


FIG. 4: (color online). The three t_{2g} orbitals corresponding to the crystal field levels shown in figure 3 for monoclinic phase of CaV_2O_4 . The orbitals (a), (b), (c) correspond to V1, (d), (e), (f) correspond to V2. The orbitals are shown in order of increasing their energy from left (the lowest in energy orbital) to right (the highest in energy orbital).

In the following, for each vanadium site i (which can be either V1 or V2) we will denote the

lowest, middle, and highest t_{2g} orbitals as ϕ_i^1 , ϕ_i^2 , and ϕ_i^3 , respectively.

The magnetic interactions are intimately connected with the spacial ordering of the t_{2g} orbitals¹³. Small structural distortions can lead to the significant changes in the orbital ordering and magnetic properties of such compounds. In the monoclinic CaV_2O_4 , there are two d electrons occupying the two lowest orbitals ϕ_i^1 and ϕ_i^2 . By neglecting for a while small off-centering of the vanadium ions, all VO_6 octahedra are compressed along the shortest V-O-V distance, which can be denoted as local z axis and, for V1, almost coincides with the crystallographic c axis. Then, the orbital with xy symmetry should be the lowest in energy. Indeed all ϕ_i^1 orbitals have predominantly xy character in agreement with these simple structural consideration (see figure 4). The lobes of the ϕ_i^1 orbitals on the neighboring V ions in the a direction are pointed along the leg of the zigzag chain. Hence, one could expect large transfer integrals in the legs of the zigzag chains.

The 3×3 matrices of transfer integrals $t_{ij}^{mm'}$, calculated in the local CF representation are summarized in table III and IV of supplementary material available at⁴. In these notations, i and j denote the vanadium sites, which can be of the type V1 or V2, while m runs over the CF orbitals ϕ_i^1 , ϕ_i^2 , and ϕ_i^3 . As expected, the largest transfer integrals operate between ϕ^1 orbitals in the legs of the zigzag chains ($t_{ij}^{11} = -265$ and -233 meV for the chains formed by V1 and V2, respectively). The transfer integrals between the chains are weaker, but comparable with the intrachain ones. Thus, despite the quasi-one-dimensional character of the crystal structure, the transfer integrals in CaV_2O_4 are essentially three dimensional. The same trend have been found for related quasi-one-dimensional compound NaV_2O_4 ¹¹.

In order to compute the screened Coulomb interactions in the t_{2g} band we use the following procedure¹⁰. First we apply constrained LDA to take into account the screening of atomic orbitals. Then the random-phase approximation (RPA) was employed to take into account the self-screening by the same $3d$ -electrons which participate in the formation of other bands due to the hybridization effects. The fitting of screened interactions in terms of two Kanamori parameters¹⁴ results in the following values of the intraorbital Coulomb interaction $U=3.42$ (3.46) eV and the intraatomic exchange coupling $J_H=0.63$ (0.64) eV for V1 (V2).

III. RESULTS AND DISCUSSION

A. Exchange interactions and magnetic ground state

First, we solve the obtained low-energy electron model in the mean-field Hartree-Fock approximation. For these purpose, we consider four collinear magnetic configurations, two of which, AFM2 and AFM3, was reported to be in moderate agreement with the single crystal neutron diffraction data (see figures 5.29(a) and 5.29(b) in ³). The unit cell was doubled along the a axis in order to arrange the V spin moments antiferromagnetically as was detected in the single-crystal neutron diffraction experiments^{3,12}. The sketch of the three considered AFM arrangements is shown in figure 5.

The parameters of interatomic magnetic interactions were calculated for different magnetic configurations by applying the perturbation theory expansion with respect to the infinitesimal spin rotations near the equilibrium state¹⁵. This procedure corresponds to the *local* mapping of the total energy change associated with the small rotations of spins onto the Heisenberg model

$$H = - \sum_{i>j} J_{ij} \mathbf{e}_i \mathbf{e}_j, \quad (1)$$

where \mathbf{e}_i is the direction of spin at the site i . The results of exchange interaction calculation for monoclinic CaV_2O_4 in the ferromagnetic (FM) and three AFM configurations are summarized in table V of supplementary material available at⁴. Since the degeneracy of t_{2g} orbitals is lifted by the lattice distortion, these exchange integrals only weakly depend on the type of the magnetic order in which they are calculated, that justifies the use of the spin-only model.

The leading exchange interactions $J_1^l = -19.9$ meV, $J_2^l = -13.9$ meV correspond to the strong AFM coupling along the leg of the zigzag chains and are about 7 times larger than the remaining interactions. The parameters of antiferromagnetic interactions in the zigzag-rung are $J_1^+ = -1.3$ meV, $J_1^- = -0.4$ meV and $J_2^+ = -1.6$ meV, $J_2^- = -1.6$ meV for V1 and V2, respectively. Such a behavior corresponds to the limit $J^l \gg J^\pm$, which is consistent with the analysis of experimental magnetic susceptibility data in³. Nevertheless, the interactions J_1^l and J_2^l in two different types of chains are substantially different.

The interactions between different types of the zigzag chains along c direction are ferromagnetic: $J_c^+ = 1.1$ meV and $J_c^- = 2.9$ meV. Similar interactions along b are found to

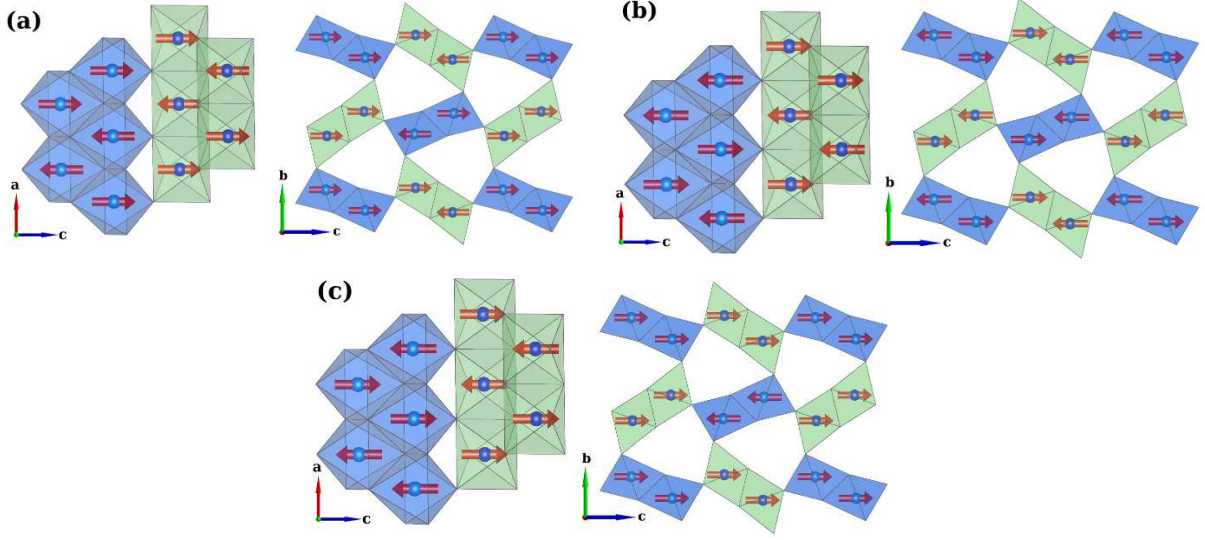


FIG. 5: (Color online). The sketch of different AFM configurations for monoclinic phase of CaV_2O_4 in the cell, doubled along a axis: AFM1 (a), AFM2 (b) and AFM3 (c).

alternate: $J_b^+ = -1.3$ meV is antiferromagnetic, while $J_b^- = 1.5$ meV is ferromagnetic. This behavior should correspond to the AFM3 magnetic alignment. This result is totally consistent with direct Hartree-Fock calculations, where the AFM3 state was found to have the lowest energy.

In order to get some insight into microscopic origin of exchange interactions, one can also estimate the parameters in the superexchange approximation, starting from the atomic limit and considering virtual hoppings to the neighboring sites in the first order of $1/U^{13,16}$. Then, J_{ij} can be calculated as the energy difference between FM ($\uparrow\uparrow$) and AFM ($\uparrow\downarrow$) configurations of spins in the bond ij : $J_{ij} = (E_{ij}^{\uparrow\downarrow} - E_{ij}^{\uparrow\uparrow})/2S^2$, where $S=1$. Since O- $2p$ and V- t_{2g} bands are separated by the large energy gap (see figure 2), we consider only the interactions caused by effective transfer integrals $t_{ij}^{mm'}$ and neglect the direct contribution of the oxygen states. In the case of CaV_2O_4 , there are two electrons residing on six spin-orbitals of t_{2g} symmetry. Therefore, in the atomic limit, two majority-spin orbitals ϕ^1 and ϕ^2 are occupied and all other orbitals (such as majority-spin ϕ^3 and all minority-spin orbitals) are empty. Then, taking into account that the hoppings are allowed only between orbitals with the same spin, we will have:

$$E_{ij}^{\uparrow\uparrow} = -\frac{t_{ij}^{13}t_{ji}^{31} + t_{ij}^{23}t_{ji}^{32}}{U - 3J_H} + (i \leftrightarrow j) \quad (2)$$

and

$$E_{ij}^{\uparrow\downarrow} = -\frac{t_{ij}^{11}t_{ji}^{11} + t_{ij}^{22}t_{ji}^{22}}{U} - \frac{t_{ij}^{12}t_{ji}^{21} + t_{ij}^{21}t_{ji}^{12} + t_{ij}^{13}t_{ji}^{31} + t_{ij}^{23}t_{ji}^{32}}{U - 2J_H} + (i \leftrightarrow j). \quad (3)$$

Using the values of transfer integrals, collected in table III and IV of supplementary material available at⁴ (note also that $t_{ij}^{mm'} = t_{ji}^{m'm}$) as well as the parameters of on-site Coulomb (U) and exchange (J_H) interactions, one can obtain that for the leg of the V1 chain: $E^{\uparrow\uparrow} = -3.34$ meV and $E^{\uparrow\downarrow} = -42.75$ meV. Therefore, $J_1^l(\text{SE})$ in the superexchange approximation can be estimated as $J_1^l(\text{SE}) = -19.7$ meV, which is in excellent agreement with $J_1^l = -19.9$ meV, obtained using the theory of infinitesimal spin rotations. For the V2 chain we obtain: $E^{\uparrow\uparrow} = -12.65$ meV and $E^{\uparrow\downarrow} = -37.89$ meV, which yield $J_2^l(\text{SE}) = -12.62$ meV, being also in good agreement with $J_2^l = -13.86$ meV, derived from the theory of infinitesimal spin rotations. Hence the difference between the leading exchange integrals for two nonequivalent types of vanadium reflects the behavior of transfer integrals. The analysis for other bonds ij can be performed in a similar way (details can be found in supplementary material available at⁴). In general, we obtain a good agreement between results of the superexchange theory and the one of the infinitesimal spin rotations.

The experimental estimations of the exchange interactions in CaV_2O_4 have been performed in two ways. On the one hand, the high temperature susceptibility data have been fitted using S=1 chain model with the nearest-neighbor and next-nearest-neighbor interactions. In notations of our paper, they corresponds to J^\pm and J^l , respectively. The solution of this model using the exact diagonalization method leads to the $J^\pm(\text{SC}) = -19.82$ meV and $J^l(\text{SC})=0^2$, which corresponds to the linear S=1 Haldane chains. The coupling between these chains was estimated to be $J_\perp/J^\pm \gtrsim 0.04$, which corresponds to $|J_\perp(\text{SC})| \gtrsim 0.8$ meV. Shortly after, similar fitting revealed two possible solutions with $J^\pm(\text{SC}) = -19.85$ meV, $J^l(\text{SC}) = -0.75$ meV and $J^\pm(\text{SC}) = -3.02$ meV, $J^l(\text{SC}) = -18.60$ meV³. In fact these two solutions are magnetically equivalent: in the first case $J^\pm(\text{SC})$ prevails and the single spin-1 chain is realized, while in the second case $J^l(\text{SC})$ is dominant, that corresponds to the formation of two independent spin-1 chains. This illustrates the fact that the fitting of the magnetic susceptibility data for materials with competing magnetic interactions is not unique: different sets of parameters can lead to similar behavior of the susceptibility. The inelastic neutron scattering measurements of the magnetic excitation spectrum in single crystals might settle this issue.

The comprehensive analysis of complex spin wave spectrum obtained by inelastic neutron

scattering (INS) technique¹² in low temperature monoclinic phase of CaV_2O_4 have been carried out within linear spin-wave theory and leads to the determination of ten exchange parameters as well as two single ion anisotropy for nonequivalent V ions. The best fit to experimental INS data was obtained for the following set of magnetic couplings: $J_1^l(\text{INS}) = J_2^l(\text{INS}) = -30$ meV, $J_1^+(\text{INS}) = -11$ meV, $J_1^-(\text{INS}) = -7.9$ meV, $J_2^+(\text{INS}) = 7.8$ meV, $J_2^-(\text{INS}) = 5.7$ meV¹². The full set of parameters in comparison with the one calculated in present work can be found in table VI of supplementary material available at⁴. These results show that the leading exchange interaction is along the leg of the zigzag chains, that partly resolve the controversy with the fitting of the magnetic susceptibility data. However, the value of the leg coupling $J^l(\text{INS}) = -30$ meV obtained within the spin-wave model¹² is about 40% larger than the one derived from the fitting of the susceptibility data $J^l(\text{SC}) = -18.60$ meV³. Moreover, the exchange interactions in zigzag rungs are rather strong $|J_{1,2}^\pm(\text{INS})| \approx 5.7\text{-}11$ meV, while the values defined by the susceptibility fitting are much smaller $|J^\pm(\text{SC})| = 3.02$ meV. Thus, it is clear that there is some controversy in the analysis of exchange interactions derived from the magnetic susceptibility and inelastic neutron scattering measurements.

To summarize this section, our theoretical value of the exchange integral $J_1^l = -19.9$ meV (for the V1 chain) is in excellent agreement with the value obtained by the fitting of susceptibility data^{2,12}. Although calculated exchange parameters $|J_{1,2}^\pm| \approx 0.4\text{-}1.6$ meV are somewhat smaller than the ones estimated from the susceptibility fitting $|J^\pm(\text{SC})| = 3.02$ meV, the general tendency $|J_{1,2}^l| \gg |J_{1,2}^\pm|$ is maintained. The exchange interaction between different zigzag chains $|J_{b,c}^\pm| \approx 1.05\text{-}2.9$ meV are also consistent with the estimation based on the susceptibility fitting $J_\perp \approx 1$ meV¹². Nevertheless, our theoretical calculations reveal a strong difference of exchange interactions in the legs of two crystallographically inequivalent chains: $J_1^l = -19.9$ meV and $J_2^l = -13.9$ meV. It is also worth to mention that the experimental and theoretical exchange interactions seem to evidence against the ladder model ($J^l, J^+ \gg J^-$) for the monoclinic phase of CaV_2O_4 .

B. Susceptibility

In order to compare the obtained values of the exchange interactions with experiment we first solve the next-nearest-neighbor spin-1 chain Heisenberg model separately for V1 and V2

using exact diagonalization (ED) method implemented in the ALPS simulation package¹⁷. In these calculations, for the nearest-neighbor interactions in the chain i , we use the averaged value of J_i^+ and J_i^- ; and for the next-nearest-neighbor interactions, we use J_i^l . By doing so, we actually simulate the behavior of the orthorhombic phase, which is realized above 141 K and for which $J_i^+ = J_i^-$. The L=12 spins along the chain were taken into account. From figure 6(a) one can see that the behavior of the single V1 chain with the leading exchange $J_1^l = -19.9$ meV agrees with experimental data very well, in agreement with results of³. Since the $J_2^l = -13.9$ meV is substantially smaller than J_1^l , the susceptibility for the V2 chain is overestimated. By considering these two noninteracting with each other zigzag chains, the total susceptibility should be obtained by averaging the data for the individual chains. Because of the V2 contribution, the obtained susceptibility deviates considerably from the experimental one below 500 K (see figure 6(b)), indicating that probably the model of two noninteracting alternating chains is not appropriate for CaV_2O_4 .

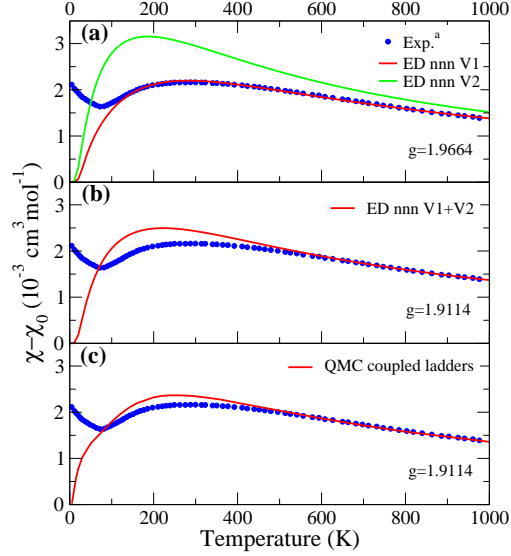


FIG. 6: (color online). The comparison of experimental static magnetic susceptibility $\chi - \chi_0$ ($\chi_0 = 0.48 \times 10^{-3} \text{ cm}^3/\text{mol}$ – temperature independent contribution) from^{3,12} ($H \parallel c$) shown as blue dots with the solution of Heisenberg model with calculated values of exchange interactions. Panel (a): comparison with ED solution of next-nearest-neighbors chains of V1 and V2 (red and green curves, correspondingly). Panel (b): comparison with the sum of two chains (red curve). Panel (c): comparison with the QMC solution of the coupled ladders model (red curve).

Then, we try to take into account the interactions between different chains and solve a more complex model using quantum Monte-Carlo method implemented in the ALPS simulation package^{17,18}. Because of the complexity of the problem (the existence of two inequivalent chains and different types of interactions between the chains) we have to rely on additional simplifications. First, we neglect the contributions of small and alternating (FM and AFM) interactions J_b^\pm . As the result, the problem is reduced to the analysis of a two-dimensional model. Then, we consider the ladders, consisting of two different interactions, J_1^l and J_2^l , in two legs of this ladder, and take into account the strongest interchain interaction $J_c^- = 2.9$ meV as the rung of the ladder. Finally, we consider the interaction between these ladders. For these purpose we use the average value of four parameters: J_1^+ , J_1^- , J_2^+ , and J_2^- . The results of these simulations are shown in figure 6(c). The considered two-dimensional model substantially improves the agreement with the experimental data and reproduces the wide peak of susceptibility at around 250 K. The values of the g -factor (1.996 and 1.911), obtained from the fitting of calculated susceptibility to the experimental data are within the typical data range $1.92 \leq g \leq 2.00$ used for the vanadium compounds and the value 1.958 obtained from Curie-Weiss fitting of the experimental susceptibility in³.

IV. CONCLUSIONS

The electronic structure, orbital configuration and magnetic interactions of quasi-one-dimensional antiferromagnet CaV_2O_4 was studied. For these purpose, the Hubbard-type model for t_{2g} states have been constructed with all the parameters derived from the first-principles calculations. The crystal field splitting and the orbital order is found to be different for two types of crystallographically inequivalent vanadium atoms. This affects the behavior of interatomic exchange interactions, which is found to be different, in several respects, from the phenomenological picture solely based on the analysis of the crystal structure of CaV_2O_4 and fitting of the experimental magnetic susceptibility. Particularly, we have found that the exchange interactions in two crystallographically inequivalent zigzag chains behave rather differently. Furthermore, there is a substantial interaction between the zigzag chains, which is comparable with intrachain interactions. This analysis allowed us to resolve several controversial issues, regarding the leading exchange interactions in CaV_2O_4 and the relative roles played by the intrachain and interchain interactions. Moreover, we argues that the

interaction between the zigzag chains is an important ingredient of realistic spin model, which should be taken into account, for instance, in the analysis of magnetic susceptibility data.

Acknowledgements

The authors thank Prof. D. C. Johnston, B. Lake and O. Pieper for providing the comprehensive information on crystal and magnetic structure of CaV_2O_4 . This work is supported by the project 14-12-00306 of the Russian Scientific Foundation. The part of the calculations were performed on the “Uran” cluster of the IMM UB RAS.

References

-
- * Electronic address: pzv@ifmlrs.uran.ru
- † Electronic address: SOLOVYEV.Igor@nims.go.jp
- ¹ Kikuchi H, Chiba M and Kubo T 2001 *Can. J. Phys.* **79** 1551
- ² Niazi A *et al.* 2009 *Phys. Rev. B* **79** 104432
- ³ Pieper O *et al.* 2009 *Phys. Rev. B* **79** 180409
- ⁴ Supplementary materials
- ⁵ Bertaut E F and van Nhung N and Hebd C R 1967 *Seances Acad. Sci. B* **264** 1416
- ⁶ Hastings J M, Corliss L M, Kunnmann W and La Placa S 1967 *J. Phys. Chem. Solids* **28** 1089
- ⁷ Sugiyama J, Ikeda Y, Goko T, Ansaldo E J, Brewer J H, Russo P L, Chow K H and Sakurai H 2008 *Phys. Rev. B* **78** 224406
- ⁸ Zong X, Suh B J, Niazi A, Yan J Q, Schlagel D L, Lograsso T A and Johnston D C 2008 *Phys. Rev. B* **77** 014412
- ⁹ Momma K and Izumi F 2011 *J. Appl. Crystallogr.* **44** 1272
- ¹⁰ Solovyev I V 2008 *J. Phys.: Condens. Matter.* **20** 293201
- ¹¹ Pchelkina Z V, Solovyev I V and Arita R 2012 *Phys. Rev. B* **86** 104409
- ¹² Pieper O *Ph.D. thesis* Der Technischen Universitt Berlin (2010)

- ¹³ Kugel K I and Khomskii D I 1982 *Sov. Phys. Usp.* **25** 231
- ¹⁴ Kanamori J 1963 *Prog. Theor. Phys.* **30** 275
- ¹⁵ Liechtenstein A I, Katsnelson M I, Antropov V P and Gubanov V A 1987 *J. Magn. Magn. Matter.* **67** 65
- ¹⁶ Anderson P W 1959 *Phys. Rev.* **115** 2
- ¹⁷ Bauer B *et al.* (ALPS collaboration) 2011 *J. Stat. Mech.* P05001; Albuquerque A F *et al.* (ALPS collaboration) 2007 *Journal of Magnetism and Magnetic Materials* **310** 1187
- ¹⁸ Alet F, Wessel S and Troyer M 2005 *Phys. Rev. E* **71** 036706